Chemical Reactions and Adsorption Geometries of Pyrrole on Ge(100)

ARTICLE *in* THE JOURNAL OF PHYSICAL CHEMISTRY B · MAY 2006

Impact Factor: 3.3 · DOI: 10.1021/jp0521656 · Source: PubMed

6 AUTHORS, INCLUDING:

Suklyun Hong
Sejong University
92 PUBLICATIONS **1,162** CITATIONS

SEE PROFILE

Chemical Reactions and Adsorption Geometries of Pyrrole on Ge(100)

Do Hwan Kim,[§,†,‡] Dae Sik Choi,[§,†] Ansoon Kim,[†] Sung-Soo Bae,[†] Suklyun Hong,*[,‡] and Sehun Kim*[,†]

Department of Chemistry and School of Molecular Science (BK 21), Korea Advanced Institute of Science and Technology, Daejeon 305-701, Republic of Korea, and Department of Physics and Institute of Fundamental Physics, Sejong University, Seoul 143-747, Republic of Korea

Received: April 16, 2005; In Final Form: January 27, 2006

The adsorption structures of pyrrole (C_4H_5N) on a Ge(100) surface at various coverages have been investigated with both scanning tunneling microscopy (STM) and ab initio density-functional theory (DFT) calculations. Three distinct features are observed in the STM images at low coverages. The comparison of the STM images with the simulation reveals that the most dominant flowerlike feature with a dark side is that the adsorbed pyrrole molecules with H dissociated form bridges between two down Ge atoms of neighboring Ge dimer rows through N−Ge bonding and β-carbon−Ge interaction. The flowerlike feature without a dark side is also observed as a minority, which is identified as nearly the same structure as the most dominant one where a dissociated H is out of the feature. The third feature showing bright protrusions may be due to a C- and N-end-on (CN) configuration, where the pyrrole molecule is located on one dimer row. At higher coverages, the number of localized configurations increases.

Introduction

Recently, there has been much attention given to the attachment of aromatic organic molecules to the surface of group IV semiconductors due to its potential applications in chemical and biological sensors, optical devices, thin film displays, and molecular electronics.[1−3] To improve the performance of molecular scale devices and maintain their molecular properties, it is important to produce organic layers on the semiconductor surface that are well-defined at the atomic scale and to understand the interface structure of the organic−semiconductor hybrid system.

One of important goals in the field of molecular electronics is the development of well-defined organic layer and chemical attachment of aromatic organic molecules to surfaces without the loss of the π conjugation.[3] Previous studies have shown that the adsorption of simple aromatic compounds such as benzene,[4] toluene,[5] and xylene[6] are accompanied by a loss of aromaticity. However, some substituted aromatic molecules such as styrene,[7] phenyl isothiocyanate,[8] and benzonitrile[9] preserve their aromaticity during adsorption because bonding through the external substituted group is favored over bonding through the aromatic ring. Therefore, it is important to understand the interfacial structures between semiconductors and organic materials in order to fabricate well-ordered organic layers.

Molecules containing nitrogen atoms are of particular interest because the lone-pair electrons are good electron donors, giving these compounds useful chemical and electrical properties. These molecules are important in the field of biological application because amine groups may be used for the attachment of biomolecules such as DNA to the surface.

Pyridine (C_5H_5N), a six-membered aromatic compound in which one C−H unit is replaced by nitrogen, adsorbs molecularly through the formation of Ge−N dative bonding and also preserves their aromaticity.[10,11] Pyrimidine ($C_4H_4N_2$) with two nitrogen atoms binds to down-Ge atoms of the adjacent dimer row via double dative bonding.[12]

Pyrrole is an aromatic molecule with one nitrogen atom that is part of a five-membered ring. In this molecule, two lone-pair electrons of the nitrogen atom and four π-electrons form a conjugated π-electron system. The pyrrole molecule could be interesting for molecular electronic applications because polypyrrole has been shown to be a good organic conductor.[13] In addition, the silicon surface covered with polypyrrole is used for "gene tip" technologies, where biological information is gained with use of polypyrrole DNA chips.[14]

Concerning the interaction of pyrrole molecules with Ge(100) and Si(100), there are many possible reaction types due to its different functional groups as shown in Figure 1: (1) The lone-pair electrons of the nitrogen atom in a pyrrole molecule can be donated into the electron-deficient down-Ge atom in a Ge dimer via dative bonding, which has been found in the reactions of aliphatic amines on a Ge surface (Figure 1a).[15] (2) The resonance structure of a pyrrole ring can lead to another dative bonding site, α- or β-carbon atom (Figure 1b,c). (3) Dissociative adsorption after N−H bond cleavage can occur preserving the ring aromaticity in the resulting reaction products (Figure 1d,e). The dissociated hydrogen atom can bind to a nearby Ge atom. This type of reaction has been found for aniline on Si(100).[16] (4) The resonance structure enables C−H dissociative adsorption at the α- or β-carbon atom (Figure 1f,g).[15] (5) Dissociative adsorption products at both the N−H and C−H bonds of the pyrrole ring have been suggested as the most stable geometry for pyrrole on Si(100) (Figure 1h,i).[17,18] (6) The pyrrole molecules having conjugated dienes can adsorb on the semiconductor surface via cycloaddition. Cycloaddition between the π-conjugated system and the Ge or Si dimer has been reported as a main reaction pathway for many aromatic molecules.[2,19] The reactions proceed in either [4+2] Diels−Alder reaction (Figure 1j) or [2+2] cycloaddition (Figure 1k).

* Corresponding authors. Suklyun Hong: e-mail hong@sejong.ac.kr. Sehun Kim: e-mail sehun-kim@kaist.ac.kr.
§ Co-first authors.
† Korea Advanced Institute of Science and Technology.
‡ Sejong University.

10.1021/jp0521656 CCC: $30.25
Published on Web 03/25/2006

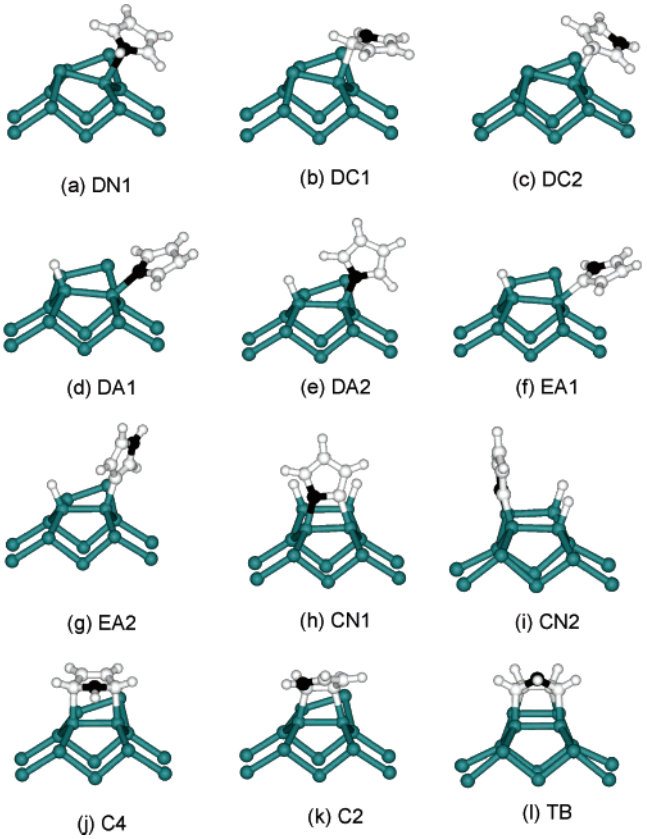

Figure 1. The possible adsorption structures of pyrrole on Ge(100) surface: (a) N-end-on dative bonding, (b) α-C-end-on dative bonding, (c) *β*-C-end-on dative bonding, (d) N−H dissociative adsorption where the pyrrole ring is tilted to the Ge surface, (e) N−H dissociative adsorption where the pyrrole ring is perpendicular to the Ge surface, (f) α-C−H dissociative adsorption, (g) *β*-C−H dissociative adsorption, (h) C- and N-end-on with on-top configuration, (i) C- and N-end-on with end-bridge configuration, (j) [4+2] cycloaddition, (k) [2+2] cycloaddition, and (l) tight-bridge structure. White, black, and blue balls represent C, N, and Ge atoms, respectively, while hydrogen atoms are represented by small white balls.

Two-step cycloaddition reactions including [2+2] following [4+2] reaction can occur to make a tight-bridge structure (Figure 1*l*).

Many experimental and theoretical results have been reported for pyrrole on Si(100).[17,18,20] But little phenomena has been elucidated for the adsorption of pyrrole on Ge(100). The interaction of organic molecules with the Ge(100) surface has received attention due to the different reactivity on Ge(100) compared with that on Si(100). The Si(100) and Ge(100) surfaces have very similar atomic structures, but the slight differences in their lattice constants and electronic structures cause different reactivity on the two surfaces.

In this work, we report STM and DFT studies of the initial adsorption structures of pyrrole on the Ge(100) surface. By comparison of the experimental STM images with the simulation, we identify three distinct features observed in the STM images at low coverages. We discuss the population change of adsorption structures as a function of pyrrole coverage.

Experimental and Theoretical Methods

Experimental Details. All experiments were performed in the ultrahigh vacuum (UHV) chambers at a base pressure below 1.0×10^{-10} Torr. One UHV chamber was equipped with a differentially pumped quadrupole mass spectrometer (QMS), an Auger electron spectroscopy (AES), low energy electron diffraction (LEED) optics, an ion sputter gun for sample cleaning, and a doser with a hexagonal array of seven parallel capillaries. The other chamber was equipped with a scanning tunneling microscope and a load-lock entry system that can transfer samples and tips. A Ge(100) sample (0.1×0.39 Ωcm, p-type, B-doped) was cleaved to a size of 2×10 mm^2 and mounted between two tantalum foil clips for STM measurements. The Ge(100) surface was cleaned by using several cycles of sputtering with 1 keV Ar^+ ions for 30 min at 700 K, followed by annealing at 900 K for 10 min. The cleanliness of the Ge(100)-2×1 surface was checked with AES. Surface impurities were found below the detection level. The (2×1) structure of the Ge(100) surface was confirmed by LEED and STM. Pyrrole (99.5% purity) purchased from Aldrich was further purified by using the freeze−pump−thaw cycles before being exposed onto the Ge(100) substrate at room temperature through a variable leak. The purity of pyrrole was checked by gas chromatography and in situ mass spectrometry. The pressure during pyrrole exposure was measured by using the ion gauge reading. The direct doser with seven capillary arrays was used to reduce the chamber background pressure. All STM measurements were performed on an OMICRON VT-STM at room temperature with subsequent annealing in a vacuum. In the STM measurements, pyrrole was exposed onto the clean Ge(100) surface for various exposure times with the chamber pressure maintained at 1×10^{-8} Torr. All STM images were recorded at a sample voltage between −1.0 and −2.0 V with a tunneling current of 0.1 nA, using electrochemically etched W-tips.

Theoretical Calculations. To investigate the configuration of pyrrole on the Ge(100) surface we have performed ab initio calculations within the local density approximation (LDA) using the Vienna ab initio simulation package (VASP).[21] Plane waves up to an energy of 224.5 eV are included to expand the wave functions, and the atoms are represented by ultrasoft pseudopotentials, as provided by VASP.[22] For bulk Ge, we determine an equilibrium lattice constant of 5.634 Å, which is in good agreement with the experimental value (5.658 Å). The pyrrole-adsorbed Ge(100) surface is modeled by a slab with a $c(4 \times 2)$ surface supercell that is composed of an adsorbed pyrrole molecule (0.25 ML), six Ge atomic layers, and an H passivating layer. The Ge bottom layer is passivated by two H atoms per Ge atom. The topmost four layers of the slab as well as the adsorbed molecules are allowed to relax by the calculated Hellmann−Feynman forces, and the remaining two Ge layers were kept frozen during the structure optimization. The surface structure is considered to be in equilibrium when the Hellmann−Feynman forces are smaller than 0.02 eV/Å. For the Brillouin-zone integration, we use a $4 \times 4 \times 1$ grid in the Monkhorst−Pack special point scheme. A Gaussian broadening with a width of 0.02 eV was used to accelerate the convergence in the *k*-point sum. With the use of the self-consistent Kohn−Sham eigenvalues and wave functions, the constant-current STM images are simulated within the Tersoff−Hamann scheme.[23] The tunneling current $I(\mathbf{r},\pm V)$ is proportional to the energy-integrated local density of states:

$$I(\mathbf{r},\pm V) \propto \sum_{n\mathbf{k}} \int_{E_F}^{E_F \pm V} |\psi_{n\mathbf{k}}(\mathbf{r})|^2 \delta(E - E_{n\mathbf{k}})\, \mathrm{d}E$$

where $+V$ and $-V$ represent the sample bias voltages for empty-state and filled-state measurements, respectively.

Results and Discussion

Figure 2a shows the filled-state STM image of a clean Ge(100) surface. The image shows a defect-free Ge(100) surface

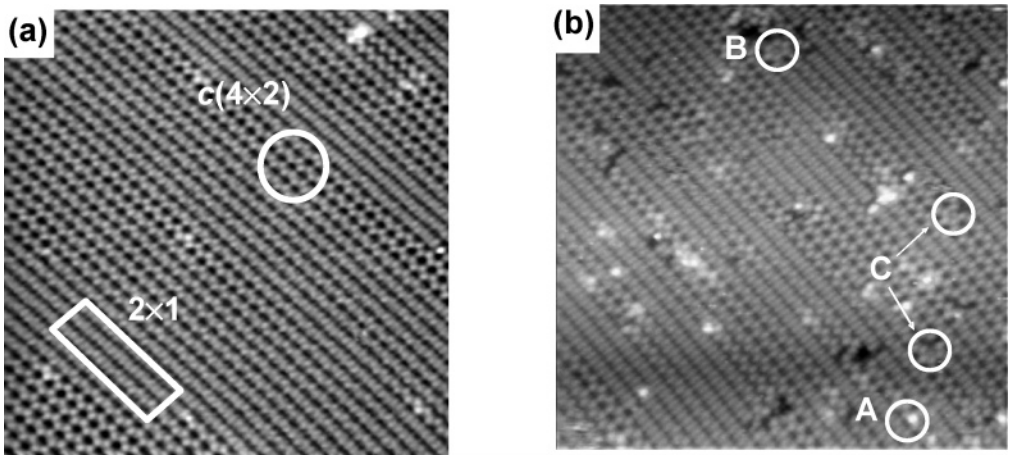

Figure 2. The STM images ($V_s = -1.7$ V, $I_T = 100$ pA, 25×25 nm^2) of (a) the clean Ge(100) surface and (b) the pyrrole adsorbed surface ($\theta = 0.027$ ML) at room temperature. Three distinct features (A, B, C) are shown in part b. For an explanation of those features, see the text.

TABLE 1: Relative Energies, ΔE (eV/molecule), of the Possible Adsorption Configurations of Pyrrole on Ge(100) with a $c(4 \times 2)$ Unit Cell[a]

	dative bonding			N−H dissociative adsorption			C−H dissociative adsorption		C- and N-end-on		cycloaddition		
	DN1	DC1	DC2	DA1	DA2	DA3	EA1	EA2	CN1	CN2	C4	C2	TB
ΔE	0.73	0.34	0.37	0.05	0.32	0	0.16	0.39	0.22	0.16	0.49	0.79	0.64

[a] The abbreviated symbols for optimized structures are shown in Figure 1 and Figure 8. The energy (ΔE) values are referred to the total energy of the tilted N−H dissociative adsorption model (DA3) in Figure 8a embedded in the $c(4 \times 2)$ unit cell. The energies are not shown for all the calculated configurations, but for relatively stable ones for each reaction type.

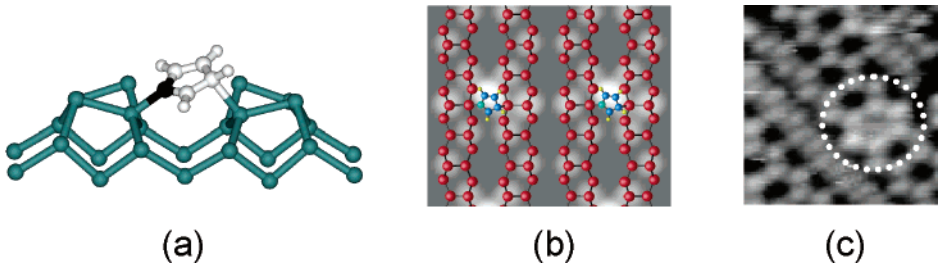

Figure 3. (a) Optimized NH dissociative configuration, where the dissociated H is diffused away (and so considered to be removed), with a $p(4 \times 4)$ unit cell. The plane of the pyrrole ring is tilted (36°) to the Ge surface. (b) Theoretical filled-state (−2.0 V) STM image for this configuration and (c) experimental STM image (feature B in Figure 2b) showing flowerlike images.

with reconstructed structures consisting of asymmetric $c(4 \times 2)$ (circle) and symmetric (2×1) dimer rows (square).

In situ STM images were obtained during the exposure of pyrrole molecules onto the clean Ge(100) surfaces at room temperature (Figure 2b). As pyrrole molecules are exposed to the Ge(100) surface, three different types of adsorbed features appear during scanning. Feature A in Figure 2b appearing as the bright protrusions is similar to that observed in the adsorption of pyrrole on Si(100).[20] Feature B looks flowerlike, which is similar to what was observed in the adsorption of pyridine on Ge(100).[10] The last feature C appears similar to feature B except that one of the hexagonal bright dots in the flowerlike structure has disappeared. Compared to the STM images of pyrrole on Si(100),[20] features B and C are newly observed. At low coverages, it is found that feature C is the most dominant among the three distinct features (see Figure 9 for the population of three features as a function of pyrrole coverage).

To understand the atomic structures for three distinct features we calculate total energies for a large number of adsorption configurations. Figure 1 shows the optimized geometry for the most stable structure among each configuration category explained in the Introduction. Also, the relative energies ΔE for the configurations are given in Table 1, where the energies

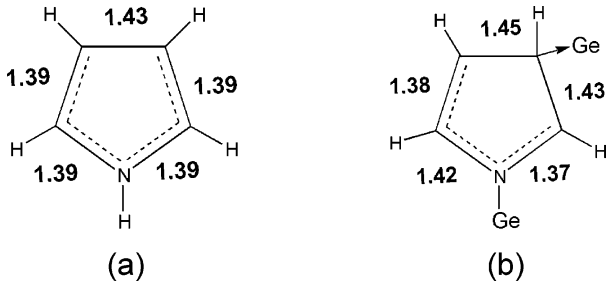

Figure 4. Optimized bond distance of the pyrrole ring: (a) pure pyrrole molecule and (b) after N−H dissociative adsorption on Ge(100) surface.

ΔE are referred to the most stable configuration among all the structures considered in this study. On the basis of the energetics and simulated STM images, we assign model configurations to the observed STM images. Note that more dominant features have lower energies.

The bright spots in a flowerlike feature B represent six up-Ge atoms of adjacent dimer rows, and a pyrrole molecule. The amount of feature B in Figure 2b is smaller than that of feature A or C. There are two possible adsorption structures for this feature B. (1) The configurations (Figure 1a−c) related to dative bonding suggested in pyridine[10] or pyrimidine[12] adsorbed on

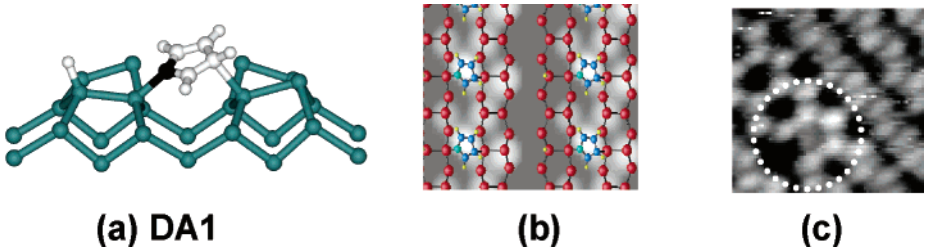

Figure 5. (a) Optimized configuration for the N−H dissociative adsorption (DA1) with a $p(4 \times 2)$ unit cell at the 0.125 ML pyrrole coverage, where the dissociated hydrogen is bound to the up-Ge atom in the same dimer. The plane of the pyrrole ring is tilted (41°) to the Ge surface. (b) Theoretical filled-state (−1.8 V) STM image for the DA1 configuration and (c) experimental STM images (feature C in Figure 2b) showing flowerlike images with a dark site.

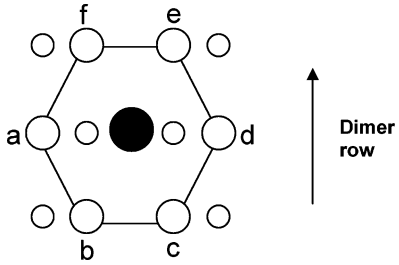

Figure 6. Possible positions (large open circles) of a dark site in feature C in Figure 2b are indicated by the letters a−f. Filled circles represent the adsorbed pyrrole molecule, while small open circles represent buckled-down Ge atoms.

Ge(100) may be a candidate. But as shown in Table 1, dative bonded configurations are all unstable compared with the NH dissociated product, so the possibility of dative bonding can be excluded. (2) The NH dissociated configuration can be another candidate for feature B. Because the pyrrole molecule is slightly acidic ($pK_a = 23.0$ in DMSO[24]), the NH dissociation before the reaction with the Ge surface may be probable. The H-dissociated pyrrole is bonded to the down-Ge atom as shown in Figure 1d, where the pyrrole ring is not restricted to the top of one dimer row, but is located between two dimer rows. The dissociated hydrogen atom might diffuse away to bond to some other Ge atoms outside the hexagon of a flowerlike feature. For simulation of the exact STM images, this dissociated hydrogen is considered to be removed from the region of interest. As a result, the filled-state STM image simulated from the H-removed NH dissociative adsorption configuration (Figure 3b) by using a $p(4 \times 4)$ unit cell[25] is found to be in good agreement with the experimentally observed flowerlike feature (Figure 3c). On the other hand, if hydrogen atom is bonded to another Ge atom inside the hexagon, a flowerlike feature with a dark side would appear, which will be discussed below in relation to feature C.

The population of feature C in Figure 2b is higher than that of feature B. Feature C is similar to feature B except that one of the bright hexagonal dots appears dark. The comparison of the STM images with the simulation reveals that feature C, the most dominant flowerlike feature with a dark side, is identified to be a N−H dissociated adsorption product (DA1 in Figure 1) where the pyrrole ring is slightly tilted to the Ge surface and bridges between two Ge dimer rows. Indeed, the DA1 configuration is found to be very stable among all the geometries considered in this study as shown in Table 1. The calculated β-C−Ge bond length (2.27 Å) is slightly longer for chemical bonding, but close enough to have weak chemical or physical interactions. The core spot in feature B of Figure 2b is not so bright as that in feature A, suggesting the change of the aromaticity in the pyrrole ring. The calculated bond distance in the pyrrole ring (Figure 4b) indicates that the aromaticity of the pyrrole ring is slightly diminished. Note that the resonance energy of the pyrrole molecule is 0.91 eV/molecule.[26] The destabilization due to weakening of the resonance is compensated by the interaction between the β-carbon atom and the down-Ge atom of the adjacent dimer row, which is approximated to be larger than the energy difference (0.27 eV/molecule) between N-end-on perpendicular (aromatic, no Ge−C interaction, DA2 in Figure 1e) and N-end-on tilted (less-aromatic, Ge−C interaction, DA1 in Figure 1d) structures formed from NH dissociative adsorption. In feature C the dark site may be attributed to the Ge atom to which the dissociated hydrogen atom is bonded. The theoretical STM image (Figure 5b) generated from the DA1 configuration by using a $p(4 \times 2)$ unit cell[25] is in good agreement with the experimental image (Figure 5c). This dark site in the DA1 configuration corresponds to the *a* or *d* position in Figure 6. But in some features, the dark sites are located in positions other than position *a* or *d*. In these cases, the dissociative adsorption product comes from the end-bridge type of reaction forming the structure shown in Figure 7. When the hydrogen is bonded, the buckling angle of the dimer decreases from 10.7° to 3.8° to give a rather symmetric dimer, which makes the dimer become dark compared to up-Ge atoms in the STM images. The structural parameters for the H-dissociated pyrrole in DA3 are almost the same as those in DA1. Note that the energy difference between DA3 and DA1 is only

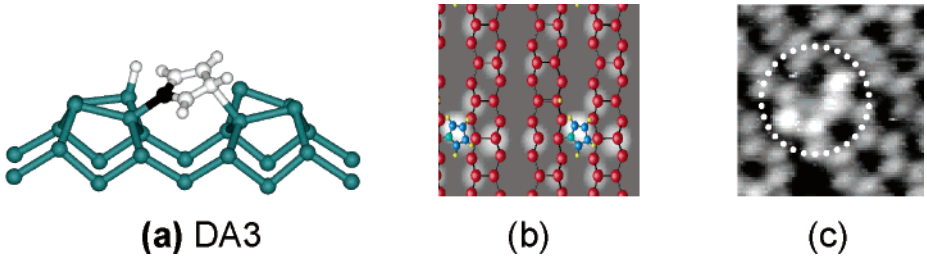

Figure 7. (a) Optimized configuration for the N−H dissociative adsorption with a $p(4 \times 2)$ unit cell, where the dissociated hydrogen is bound to a Ge atom of the next dimer in the same dimer row. The plane of the pyrrole ring is tilted (36°) to the Ge surface. (b) Theoretical filled-state (−1.8 V) STM images for the DA3 configuration, where a $p(4 \times 4)$ unit cell is used to simulate the exact features shown in the experimental STM images. (c) The experimental image (feature C in Figure 2b) showing flowerlike images with a dark site.

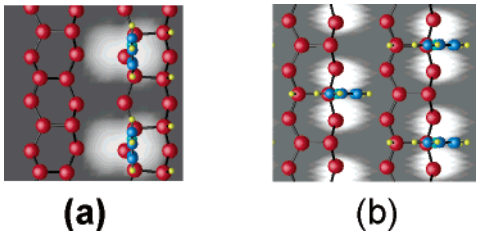

Figure 8. Theoretical filled-state (−1.8 V) STM images for (a) CN2 and (b) DA2 configurations.

0.05 eV/molecule for a $c(4 \times 2)$ unit cell as shown in Table 1. The theoretical STM image (Figure 7b) generated from DA3 by using a $p(4 \times 4)$ unit cell[25] explains well the experimental image (Figure 7c).

Meanwhile, the electrophilic aromatic substitution product (EA1 in Figure 1f) resulting from C−H dissociation shows a simulated STM image (not shown here) similar to that for DA1, and is 0.11 eV/molecule higher in energy than DA1. Thus it will also contribute to feature C in Figure 2b as a minority.

Most of the adsorption features A of Figure 2b showing bright protrusions seem to be located on either the right or the left side of a dimer row. Since the simulated STM images show a bright protrusion even for the somewhat perpendicularly aligned pyrrole molecule on the surface, we may have various candidates for the bright protrusions. However, on the basis of the energetics, we may exclude the perpendicular configurations such as H-dissociated DA2. Among the possible geometries where the pyrrole molecule is located on the dimer row, an end-bridged type of the C- and N-end-on (CN2) configuration (Figure 1i) involving both C−H and N−H dissociative adsorption is relatively stable. The theoretical STM images generated from CN2 (Figure 8a) show bright protrusions similar to feature A, implying that CN2 may be a possible candidate for bright protrusions. In accordance with energetic consideration, the simulated STM image from DA2 results in a different adsorption feature (Figure 8b). The arrangement and size of bright protrusions are variable, so the details will be studied elsewhere.

Figure 9 shows the filled-state STM images as a function of pyrrole coverage. The series of STM images was recorded during real-time dosing of pyrrole onto the Ge(100) surface. Four STM images taken on the same surface region (25×25 nm^2) show three different features as mentioned above. As the coverage of pyrrole increases, the STM images show that the number of bright protrusions increases.

Figure 10 shows the population of three different adsorption features as a function of pyrrole coverage, which are measured by directly counting the number of each feature in the STM images. The populations were averaged over the STM images of three different surface regions and normalized by the coverage of adsorbed pyrrole molecules. The STM images above 0.2 ML of pyrrole were not used for counting because of the difficulty in distinguishing three different features at high exposure of pyrrole. The number of features C reaches saturation around pyrrole coverage of 0.15 ML. As was mentioned above, the adsorption structure of feature C is the most stable, but requires two dimer rows. Therefore, the population of feature C would reach a maximum point as increasing pyrrole coverage. On the other hand, the population of feature A grows more rapidly than the other features B and C. This may be due to less steric hindrance in feature A compared to that in features B and C at higher coverages.

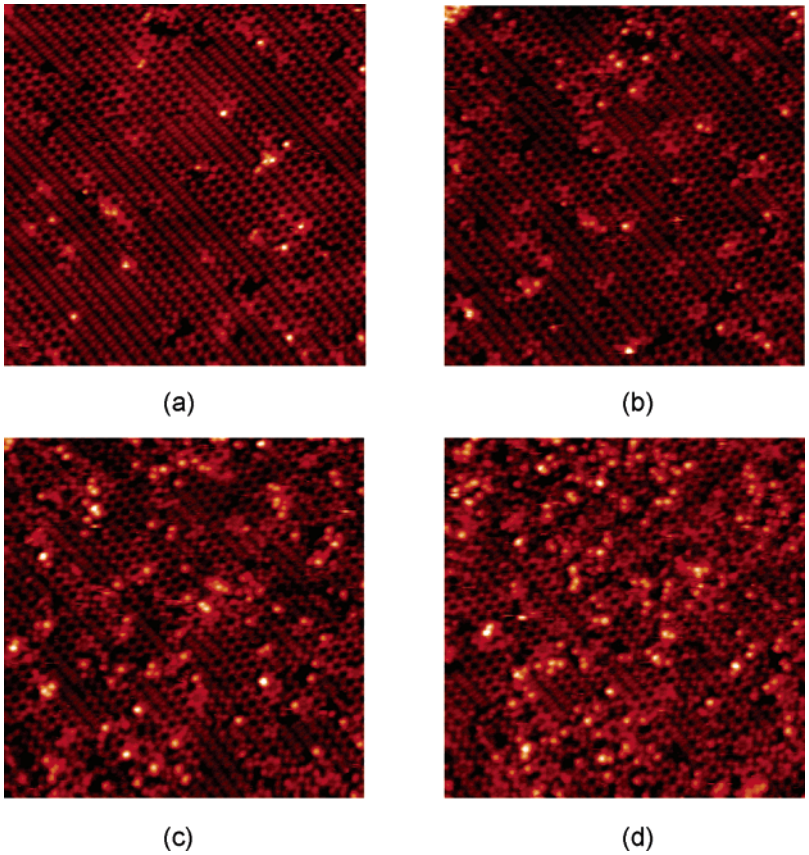

Figure 9. The filled-state STM images ($V_s = -1.7$ V, $I_T = 100$pA) taken on the same surface region (25×25 nm^2) after exposure of pyrrole: (a) 0.027, (b) 0.072, (c) 0.13, and (d) 0.18 ML of pyrrole.

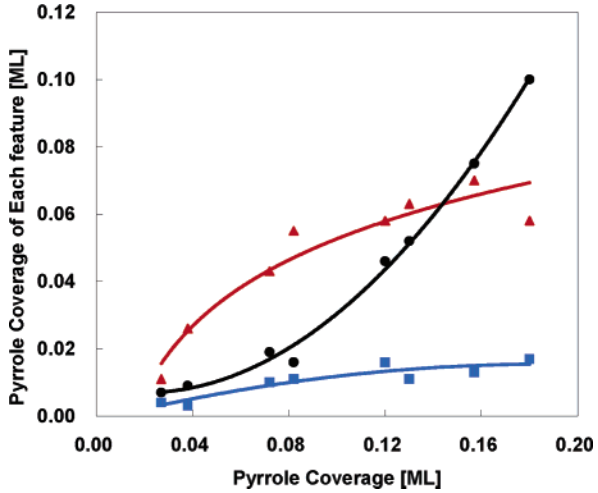

Figure 10. The population of adsorption features of pyrrole on the Ge(100) surface as a function of coverage. The number of each feature is normalized by the coverage of adsorbed pyrrole molecules. Features A, B, and C are represented by circle (black), square (blue), and triangle (red), respectively.

Conclusion

In this study, we have investigated the adsorption of a pyrrole molecule on the Ge(100) surface using STM and ab initio calculations. With use of a real-time STM, three different adsorption features of pyrrole were observed on the Ge(100) surface at room temperature. To identify three distinct STM features, we calculated total energies for many possible configurations. On the basis of energetics, comparison of the experimental STM images with the simulated ones revealed three features.

A C- and N-end-on configuration (Figure 1i) may be a possible candidate for bright protrusions in the STM images. The pyrrole molecule adsorbs on Ge dimers via Ge−N and Ge−C linkage through the dissociation of N−H and α-C−H of pyrrole, and is confined to either the left or the right side of a dimer row. The pyrrole molecules retain aromaticity, which appears as bright protrusions in the STM image.

The STM images of features B and C show a flowerlike hexagonal feature involving two adjacent Ge dimer rows and the adsorbed pyrrole molecule. Both features are found to result from the stable N-end-on tilted structures. In feature B, the H-dissociated pyrrole reacts with a down-Ge atom (Figure 3) and the dissociated H diffuses out of the region of interest. On the other hand, in feature C, the dissociated H is bonded to another Ge atom within the hexagonal feature (Figures 5 and 7). The aromaticity of the pyrrole ring is affected, because of the interaction between the β-carbon atom and the Ge atom of the adjacent dimer row.

At low coverage, adsorption feature C was mainly observed as the most stable configuration, but feature A became dominant at high coverages, due to less steric hindrance compared to other features.

Acknowledgment. This research was supported by grants from KOSEF through the Center for Nanotubes and Nanostructured Composites, the Brain Korea 21 Project, and the National R&D Project for Nano Science and Technology. The calculations were supported by the KISTI through the 6th Strategic Supercomputing Support Program.

References and Notes

(1) Yate., J. T., Jr. *Science* **1998**, *279*, 335.
(2) Wolkow, R. A. *Annu. Rev. Phys. Chem.* **1999**, *50*, 413.
(3) Cao, X.; Coulter, S. K.; Ellison, M. D.; Liu, H.; Liu, J.; Hamers, R. J. *J. Phys. Chem. B* **2001**, *105*, 3759.
(4) Gokhale, S.; Trischberger, P.; Menzel, D.; Widdra, W.; Dröge, H.; Steinrück, H. P.; Birkenheuer, U.; Gutdeutsch, U.; Rösch, N. *J. Chem. Phys.* **1998**, *108*, 5554.
(5) Borovsky, B.; Krueger, M.; Ganz, E. J. *J. Vac. Sci. Technol. B* **1999**, *17*, 7.
(6) Coulter, S. K.; Ellison, M. D.; Hamers, R. J. *J. Vac. Sci. Technol. A* **2000**, *18*, 1965.
(7) Coulter, S. K.; Ellison, M. D.; Hamers, R. J. *J. Am. Chem. Soc.* **2000**, *122*, 8529.
(8) Ellison, M. D.; Hamers, R. J. *J. Phys. Chem. B* **1999**, *103*, 6243.
(9) Tao, F.; Wang, Z. H.; Xu, G. Q. *J. Phys. Chem. B* **2002**, *106*, 3557.
(10) Cho, Y. E.; Maeng, J. Y.; Kim, S.; Hong, S. *J. Am. Chem. Soc.* **2003**, *125*, 7514.
(11) Hong, S.; Cho, Y. E.; Maeng, J. Y.; Kim, S. *J. Phys. Chem. B* **2004**, *108*, 15229.
(12) Lee, J. Y.; Jung, S. J.; Hong, S.; Kim, S. *J. Phys. Chem. B* **2005**, *109*, 348.
(13) Yang, Y.; Liu, J.; Wan, M. *Nanotechnology* **2002**, *13*, 771.
(14) Marchand, G. T.; Bidan, G.; Teoule, R.; Mathis, G. *Anal. Biochem.* **1998**, *255*, 188.
(15) Wang, G. T.; Mui, C.; Tannaci, J. F.; Filler, M. A.; Musgrave, C. B.; Bent, S. F. *J. Phys. Chem.* **2003**, *107*, 4982.
(16) Rummel, R. M.; Ziegler, C. *Surf. Sci.* **1998**, *418*, 303.
(17) Seino, K.; Schmidt, W. G.; Furthmuller, J.; Bechstedt, F. *Phys. Rev. B* **2002**, *66*, 235323.
(18) Seino, K.; Schmidt, W. G.; Furthmuller, J.; Bechstedt, F. *Surf. Sci.* **2003**, *532*, 988.
(19) Bent, S. F. *Surf. Sci.* **2002**, *500*, 879.
(20) Maeng, J. Y.; Cho, Y. E.; Jung, S. J.; Kim, S. To be submitted for publication.
(21) Kresse, G.; Furthmüller, J. *Comput. Mater. Sci.* **1996**, *6*, 15.
(22) Kresse, G.; Hafner, J. *J. Phys. Condens. Matter* **1994**, *6*, 8245.
(23) Tersoff, J.; Hamann, D. R. *Phys. Rev. Lett.* **1983**, *50*, 1998. Tersoff, J.; Hamann, D. R. *Phys. Rev. B* **1985**, *31*, 805.
(24) Bordwell, F. G.; Drucker, G. E.; Fried, H. E. *J. Org. Chem.* **1981**, *46*, 632.
(25) We calculated total energies for structures shown in Figure 1 using a $c(4 \times 2)$ surface unit cell, while we used different surface unit cells, $p(4 \times 2)$ or $p(4 \times 4)$, to simulate the exact features shown in the experimental STM images.
(26) Smith, M.; March, J. *March's Advanced Organic Chemistry: Reactions, Mechanisms, and Structure*, 5th ed.; Wiley: New York, 2001.